

Relativistic approach to one nucleon knockout reactions

Andrea Meucci,* Carlotta Giusti, and Franco Davide Pacati

*Dipartimento di Fisica Nucleare e Teorica, Università di Pavia and
Istituto Nazionale di Fisica Nucleare, Sezione di Pavia, I-27100 Pavia, Italy*

We develop a fully relativistic distorted wave impulse approximation model for electron- and photon-induced one proton knockout reactions. The relativistic mean field for the bound state and the Pauli reduction for the scattering state are used, including a fully relativistic electromagnetic current operator. Results for $^{16}\text{O}(e, e'p)$ cross section and structure functions are shown in various kinematic conditions and compared with nonrelativistic calculations. Nuclear transparency calculations in a Q^2 range between 0.3 and 1.8 $(\text{GeV}/c)^2$ are presented. Results for $^{16}\text{O}(\gamma, p)$ differential cross sections are displayed in an energy range between 60 and 150 MeV including two-body seagull contribution in the nuclear current.

PACS numbers: 25.30.Fj, 25.20.Lj, 24.10.Jv, 24.10.Eq

I. INTRODUCTION

One nucleon knockout reactions are a primary tool to explore the single-particle aspects of the nucleus. A long series of high-precision measurements at different energies and kinematics in a wide range of target nuclei stimulated the production of a considerable amount of theoretical calculations [1, 2, 3, 4, 5]. In the one-photon exchange approximation the coincidence cross section is given by the contraction between the lepton tensor, completely determined by QED, and the hadron tensor, whose components depend on the transition matrix elements of the nuclear current operator. In this note, the matrix elements of the nuclear current operator, i.e.,

$$J^\mu = \langle \Psi_f | j^\mu | \Psi_i \rangle, \quad (1)$$

are calculated with relativistic wave functions for initial and scattering states. The bound state wave functions, i.e.,

$$\Psi_i = \begin{pmatrix} u_i \\ v_i \end{pmatrix}, \quad (2)$$

are given by the Dirac-Hartree solution of a relativistic Lagrangian containing scalar and vector potentials [6]. The ejectile wave function is written in terms of its positive energy component following the direct Pauli reduction scheme, i.e.,

$$\Psi_f = \begin{pmatrix} \Psi_{f+} \\ \frac{\mathbf{p} \cdot \mathbf{V}}{M+E'+S-V} \Psi_{f+} \end{pmatrix}, \quad (3)$$

where $S = S(r)$ and $V = V(r)$ are the scalar and vector potentials for the nucleon with energy and momentum E' and \mathbf{p}' [7]. The upper component, Ψ_{f+} , is related to a

Schrödinger equivalent wave function, Φ_f , by the Darwin factor, $D(r)$, i.e.,

$$\Psi_{f+} = \sqrt{D(r)} \Phi_f, \quad (4)$$

$$D(r) = 1 + \frac{S - V}{M + E'}. \quad (5)$$

Φ_f is a two-component wave function which is solution of a Schrödinger equation containing equivalent central and spin-orbit potentials obtained from the scalar and vector potentials. The most common current conserving prescriptions, i.e., cc1, cc2, and cc3 [8], are used for the one-body current j^μ .

II. THE $(e, e'p)$ REACTION

The coincidence cross section of the $(e, e'p)$ reaction can be written in terms of four response functions, $R_{\lambda\lambda'}$, as

$$\sigma = K \{ v_L R_L + v_T R_T + v_{LT} R_{LT} \cos(\vartheta) + v_{TT} R_{TT} \cos(2\vartheta) \}, \quad (6)$$

where K is a kinematic factor, and ϑ is the out-of-plane angle between the electron scattering plane and the $(\mathbf{q}, \mathbf{p}')$ plane. The coefficients $v_{\lambda\lambda'}$ are obtained from the lepton tensor components and depend only upon the electron kinematics [1, 2].

The response functions are given by bilinear combinations of the nuclear current components, i.e.,

$$\begin{aligned} R_L &\propto \langle J^0 (J^0)^\dagger \rangle, \\ R_T &\propto \langle J^x (J^x)^\dagger \rangle + \langle J^y (J^y)^\dagger \rangle, \\ R_{LT} &\propto -2 \text{Re} \left[\langle J^x (J^0)^\dagger \rangle \right], \\ R_{TT} &\propto \langle J^x (J^x)^\dagger \rangle - \langle J^y (J^y)^\dagger \rangle, \end{aligned} \quad (7)$$

where $\langle \dots \rangle$ means that average over the initial and sum over the final states is performed fulfilling energy conservation.

*Talk presented by Andrea Meucci at the IX Workshop on Theoretical Nuclear Physics in Italy, Cortona, Italy, 9-12 October 2002

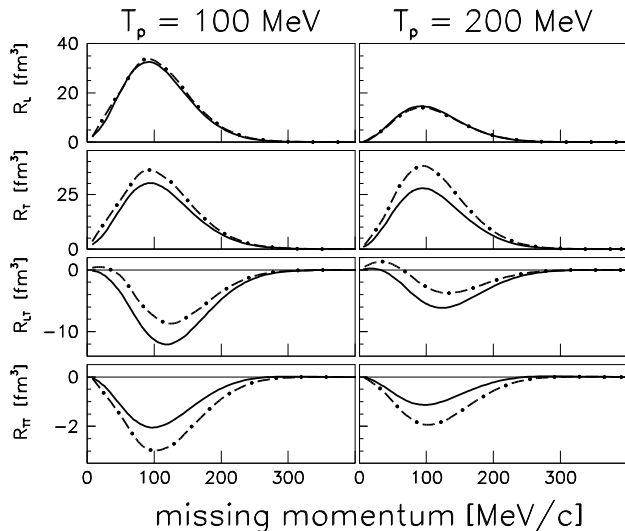


FIG. 1: The response functions for the $^{16}\text{O}(e, e'p)^{15}\text{N}$ reaction at $T_p = 100$ (left panel) and 200 MeV (right panel) in the center-of-mass system in constant (\mathbf{q}, ω) kinematics. Solid lines are the relativistic results, dot-dashed lines are the non-relativistic results.

The comparison between our relativistic distorted wave impulse approximation (RDWIA) results and the nonrelativistic results [1] is shown in Fig. 1 for the response functions of the $^{16}\text{O}(e, e'p)^{15}\text{N}_{\text{g.s}}$ reaction in constant (\mathbf{q}, ω) kinematics at two different values of the proton energy, i.e., $T_p = 100$ and 200 MeV [9]. The cc2 prescription has been used. The differences rapidly increase with the energy, and the relativistic results are smaller than the nonrelativistic ones. This outcome is well-known and it is essentially due to the \sqrt{D} factor of Eq. 5 and to the relativistic normalization factor $(M + E')/(2E')$. Small differences are obtained for the longitudinal response function R_L . On the contrary, a visible reduction is found for the transverse response R_T , even at $T_p = 100$ MeV. Large differences are generally found for the longitudinal-transverse interference response R_{LT} . The combined relativistic effects on R_T and R_{LT} are responsible for the different asymmetry in the cross section. The transverse-transverse interference response R_{TT} is much smaller than the other response functions and gives only a negligible contribution to the cross section.

In the upper panel of Fig. 2, the reduced cross section data measured at NIKHEF in parallel kinematics at a constant $T_p \simeq 90$ MeV in the center-of-mass system [10] are compared with our calculations [9, 11]. The relativistic curves have been rescaled by the spectroscopic factors $Z_{p1/2} = 0.71$ and $Z_{p3/2} = 0.60$, while the non-relativistic ones by $Z_{p1/2} = 0.64$ and $Z_{p3/2} = 0.54$. It is apparent that, at low energy, relativistic and nonrelativistic calculations are almost equivalent in comparison with data. However, the fact that the relativistic calculations are normalized to experimental data with a closer

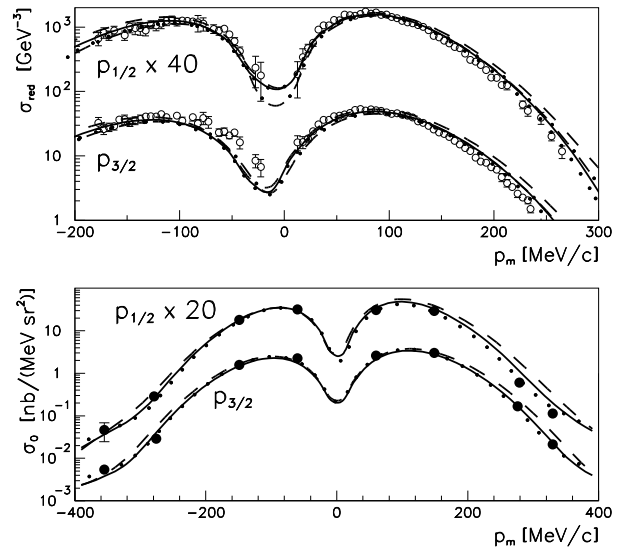


FIG. 2: The cross section for the $^{16}\text{O}(e, e'p)^{15}\text{N}$ reaction at $T_p = 90$ MeV in parallel kinematics (upper panel) [10], and at $Q^2 = 0.8$ $(\text{GeV}/c)^2$ in constant (\mathbf{q}, ω) kinematics [12] (lower panel). Data for the $p_{1/2}$ state have been multiplied by 40 and 20, respectively. Dashed, solid, and dotted lines represent the result of the RDWIA approach with cc1, cc2, cc3 off-shell prescriptions, respectively. Dot-dashed lines in the upper panel are the nonrelativistic results.

to 1 spectroscopic factor, seems to indicate that a relativistic treatment should be preferred with respect to a nonrelativistic one. The sensitivity to the off-shell ambiguity in the electromagnetic current operator is relatively weak and remains within a range of about 10%.

In the lower panel, the same reaction is considered at the Jlab constant (\mathbf{q}, ω) kinematics with $Q^2 = 0.8$ $(\text{GeV}/c)^2$ [12]. The spectroscopic factors are the same as in the upper panel. The agreement with data is still very good. We remark that, at this energy, a relativistic treatment is necessary to correctly describe the data.

III. NUCLEAR TRANSPARENCY

The nuclear transparency can be intuitively defined as the ratio of the measured to the plane wave cross section. The transparency can be used to refine our knowledge of nuclear medium effects and to look for deviation from conventional nuclear physics, such as the Color Transparency (CT) effect [13, 14, 15]. If the CT effect switches on as Q^2 increases, then the nuclear transparency should be enhanced towards unity.

Several measurements of the nuclear transparency in $(e, e'p)$ have been carried out in the past, but they did not show any evidence for the onset of CT in a Q^2 range up to 8.1 $(\text{GeV}/c)^2$.

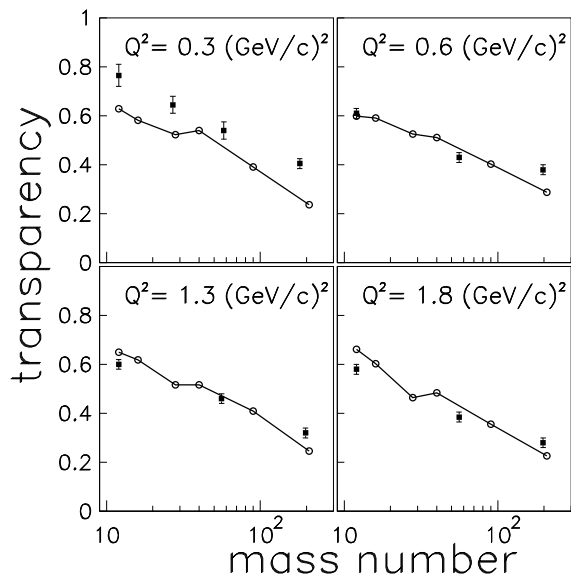


FIG. 3: The nuclear transparency for the quasifree $A(e, e'p)$ reaction as a function of the mass number for Q^2 ranging from 0.3 to 1.8 $(\text{GeV}/c)^2$. Calculations have been performed for selected closed shell or subshell nuclei with mass numbers indicated by open circles. The data at $Q^2 = 0.3 (\text{GeV}/c)^2$ are from Ref. [13]. The data at $Q^2 = 0.6, 1.3,$ and $1.8 (\text{GeV}/c)^2$ are from Ref. [14].

We define nuclear transparency as

$$T = \frac{\int_V dE_m d\mathbf{p}_m \sigma_{DW}(E_m, \mathbf{p}_m, \mathbf{p}')}{\int_V dE_m d\mathbf{p}_m \sigma_{PW}(E_m, \mathbf{p}_m)}, \quad (8)$$

where σ_{DW} is the distorted wave cross section and σ_{PW} is the plane wave one. The integration is performed upon the space phase volume V .

In Fig. 3 our RDWIA results for nuclear transparency, calculated with the *cc2* prescription for the nuclear current, are shown [16]. The Q^2 of the exchanged photon is taken between 0.3 $(\text{GeV}/c)^2$ and 1.8 $(\text{GeV}/c)^2$ in constant (\mathbf{q}, ω) kinematics. Calculations have been performed for selected closed shell or subshell nuclei. The agreement with the data is rather satisfactory. At $Q^2 = 0.3 (\text{GeV}/c)^2$ our results lie below the data, while at $Q^2 = 0.6, 1.3,$ and $1.8 (\text{GeV}/c)^2$ they are closer to the data and fall down only for higher mass numbers. The discontinuities of the shell structure clearly appear in the changes in shape of the A -dependent curves.

IV. PHOTOREACTIONS

In case of an incident photon with energy E_γ , the (γ, N) cross section can be written in terms of the pure transverse response, i.e.,

$$\sigma_\gamma = K' R_{TT}, \quad (9)$$

where K' is a kinematic factor.

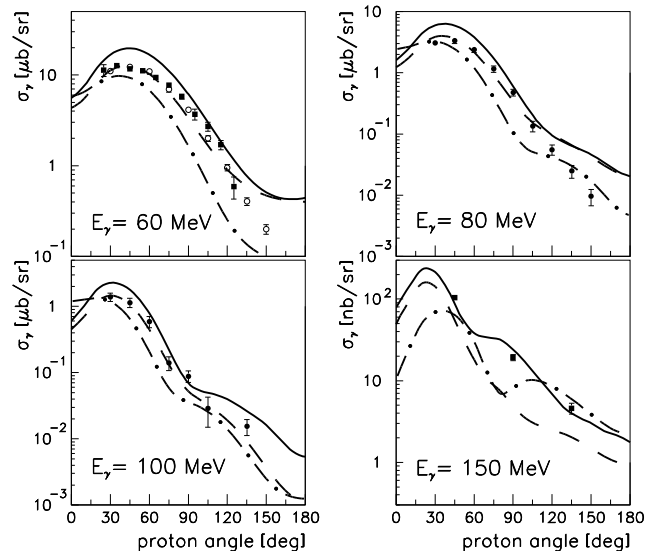


FIG. 4: The cross section for the $^{16}\text{O}(\gamma, p)^{15}\text{N}$ reaction as a function of the proton scattering angle at a photon energy ranging from 60 to 150 MeV. The data at 60 MeV are from Refs. [19, 20]. The data at 80 and 100 MeV are from Ref. [20]. The data at 150 MeV are from Ref. [21]. Solid lines represent the relativistic calculations with the inclusion of the seagull current, dashed lines the relativistic results with one-body current only, and dot-dashed lines are the one-body nonrelativistic results.

The comparison between relativistic and nonrelativistic results is shown in Fig. 4 for the cross section of the $^{16}\text{O}(\gamma, p)^{15}\text{N}_{\text{g.s.}}$ reaction at photon energy ranging from 60 to 150 MeV [17]. The *cc2* current has been used and the same spectroscopic factor $Z(p\frac{1}{2}) = 0.71$ of $(e, e'p)$ data has been applied.

We see that the differences between the nonrelativistic calculations and the relativistic ones with the *cc2* prescription are sensible at all energies. The nonrelativistic results are always smaller than the data. On the contrary, the relativistic results with the one-body current are generally closer to the data and well reproduce the magnitude and shape, at least at low energies. For higher energies, the relativistic results fall below the data and the discrepancies increase with the proton angle.

As a first step to study the role of meson exchange currents in photoreactions, the results with the inclusion of the seagull contribution in the current are also shown in Fig. 4 [18]. The pure contribution of the two-body term is one order of magnitude lower than the one-body one, but their interference is large. Thus, the total result is enhanced above the data and the shape is slightly affected. The seagull contribution is sizable but less than in previous nonrelativistic calculations [1]. On the other hand, in nonrelativistic calculations, the pion-in-flight diagram reduces the effects of the seagull current, while the Δ current is important only with increasing photon energies. If these results were confirmed in relativistic calculations,

the pion-in-flight term would reduce the contribution of seagull and bring the calculated cross section in Fig. 4 closer to the one-body results and also to the data.

-
- [1] S. Boffi, C. Giusti, F. D. Pacati, and M. Radici, *Electromagnetic Response of Atomic Nuclei*, Oxford Studies in Nuclear Physics Vol. 20 (Clarendon Press, Oxford, 1996).
- [2] J.J. Kelly, *Adv. Nucl. Phys.* **23**, 75 (1996).
- [3] Y. Jin, D. S. Onley, and L. E. Wright, *Phys. Rev. C* **45**, 1311 (1992); Y. Jin and D. S. Onley, *ibid.* **C 50**, 377 (1994);
- [4] J. J. Kelly, *Phys. Rev. C* **60**, 044609 (1999);
- [5] J. M. Udías *et al.*, *Phys. Rev. C* **48**, 2731 (1993); **C 51**, 3246 (1995); J. M. Udías *et al.*, *ibid.* **C 53**, R1488 (1996); J. M. Udías and J. R. Vignote, *ibid.* **C 62**, 034302 (2000); J. M. Udías *et al.*, *ibid.* **C 64**, 024614 (2001).
- [6] W. Pöschl, D. Vretenar, and P. Ring, *Comput. Phys. Commun.* **103**, 217 (1997).
- [7] E.D. Cooper, S. Hama, B.C. Clark, and R.L. Mercer, *Phys. Rev. C* **47**, 297 (1993).
- [8] T. de Forest, Jr., *Nucl. Phys.* **A392**, 232 (1983).
- [9] A. Meucci, C. Giusti, and F. D. Pacati, *Phys. Rev. C* **64**, 014604 (2001).
- [10] M. Leuschner *et al.*, *Phys. Rev. C* **49**, 955 (1994).
- [11] M. Radici, A. Meucci, and W. H. Dickhoff, [nucl-th/0205013](#).
- [12] J. Gao *et al.*, *Phys. Rev. Lett.* **84**, 3265 (2000).
- [13] G. Garino *et al.*, *Phys. Rev. C* **45**, 780 (1992);
- [14] D. Abbott *et al.*, *Phys. Rev. Lett.* **80**, 5072 (1998);
- [15] T. G. O'Neill *et al.*, *Phys. Lett.* **B351**, 87 (1995); K. Garrow *et al.*, [hep-ex/0109027](#).
- [16] A. Meucci, *Phys. Rev. C* **65**, 044601 (2002).
- [17] A. Meucci, C. Giusti, and F. D. Pacati, *Phys. Rev. C* **64**, 064615 (2001).
- [18] A. Meucci, C. Giusti, and F. D. Pacati, *Phys. Rev. C* **66**, 034610 (2002).
- [19] G. J. Miller *et al.*, *Nucl. Phys.* **A586**, 125 (1995).
- [20] D. J. S. Findlay and R. O. Owens, *Nucl. Phys.* **A279**, 385 (1977).
- [21] M. J. Leitch *et al.*, *Phys. Rev. C* **31**, 1633 (1985).